LA-7384-MS
Informal Report

A Catalog of Two-Dimensional Vortex Patterns

University of California
LOS ALAMOS SCIENTIFIC LABORATORY
Post Office Box 1663 Los Alamos, New Mexico 87545

LA-7384-MS
Informal Report

Special Distribution
Issued: October 1978

A Catalog of Two-Dimensional Vortex Patterns

L. J. Campbell
Robert Ziff

A CATALOG OF TWO-DIMENSIONAL VORTEX PATTERNS

by

L. J. Campbell and Robert Ziff

ABSTRACT

We list the two-dimensional patterns that correspond to minima in the free energy of identical parallel vortices inside a rotating cylinder of liquid such as superfluid ^{4}He. All known stable patterns are listed for N = 1, 2,.., 30, 37, 50, where N is the number of vortices. The two lowest energy patterns are shown for all "triangular" numbers, N = 1+6(1+2+3+..), through N = 217. For each value of N the different patterns are ordered according to their relative free energy.

I. INTRODUCTION

This report gives a more extensive and systematic list of two-dimensional stable vortex patterns than has been available heretofore. Although the results are directly applicable to studies of either the energy levels of rotating superfluid ^{4}He or dislocations in a single crystal under torsion, we use notation and terminology appropriate only to the former system.

Irreversible frictional effects (viscosity) drive normal fluids within a rotating container to a state of solid body rotation. However, the quantum nature of the superfluid component of liquid ^{4}He below 2.172 K absolutely precludes solid body rotation as a possible state of this component. Instead, superfluids react to rotating containers by generating a nearly uniform density of quantized rectilinear vortex lines, parallel to the axis of rotation,

which simulate solid body rotation very closely on a distance scale large compared to the vortex spacing. However, for systems of only a few vortices, the discrete nature of the possible rotational states becomes manifest and permits an ordering of states on the basis of vortex number and pattern symmetry.

One hundred years ago interest in the vortex theory of atoms inspired Lord Kelvin to solve the case of three vortices equally spaced on a circle; five years later, J. J. Thomson proved that up to six vortices on a circle are stable. About fifty years later, T. H. Havelock[1] proved that the presence of either an interior or exterior circular boundary caused absolute instability in a ring of seven or more vortices. More recently, Hess[2] calculated the free energy of bounded rings consisting of up to seven vortices, both with and without an additional vortex at the center. For larger numbers of vortices the free energy formula becomes analytically intractable and direct calculation is required. Stauffer and Fetter[3], the first to report computer calculations of vortex patterns inside a circular boundary, published two patterns for 37 vortices together with their associated free energies for a particular angular velocity. We extend these results both in the number of patterns calculated and in the method of assigning a unique energy number to each pattern.

Section II contains the equations used to calculate the patterns and a description of the calculational procedure. A summary of the patterns is listed in Sec. III and figures of the patterns are shown in Sec. IV.

II. EQUATIONS AND PROCEDURE

In reduced units, the free energy per unit length of N identical rectilinear vortices in a rotating cylinder is[2]

$$f = \ell n \left[\frac{\prod_{i=1}^{N} (1-r_i^2) \prod_{i=1}^{N} \prod_{j=1}^{i-1} (1 + r_i^2 r_j^2 - 2\, r_i r_j \cos\theta_{ij})}{\prod_{i=1}^{N} \prod_{j=1}^{i-1} (r_i^2 + r_j^2 - 2\, r_i r_j \cos\theta_{ij})} \right] - \omega \sum_{i=1}^{N} (1-r_i^2) + N\, \ell n(R/a) \,, \tag{1}$$

where

f = free energy in units of $\rho\kappa^2/4\pi$,

r_j = radial distance of j^{th} vortex from center of cylinder (and axis of rotation) in units of R,

$\theta_{ij} = \theta_i - \theta_j$, the angle between $\underset{\sim}{r}_i$ and $\underset{\sim}{r}_j$,

ω = reduced angular velocity of cylinder, equal to $2\pi R^2\Omega/\kappa$ where Ω is the physical angular velocity,

a = vortex core radius,

ρ = density of liquid (for helium, ρ is the superfluid density),

κ = strength of vortex (for helium, $\kappa = h/m = 0.9967\ 10^{-3}\ cm^2/s$).

The term "free energy" is used because we are interested in the equilibrium states of the system for given angular velocity ω in analogy to the usual free energy F which is appropriate to systems of given temperature, $F = E - TS$. That is, $f = e - \omega\ell$, where e and ℓ are the dimensionless kinetic energy and the angular momentum of the system in the fixed, laboratory frame. Apart from a constant, f is also the kinetic energy of the liquid in a reference frame that is rotating with angular velocity ω. In these dimensionless units, solid-body rotation of the liquid has the free energy

$$f_s = -\frac{1}{4}\omega^2 .$$

Although the temperature is important in determining the time required for a helium vortex system to reach an equilibrium pattern, it does not affect the type of pattern nor the relative energy of different patterns and therefore can be ignored here.

A vortex pattern with coordinates $[r_i, \theta_i]$ is, respectively, stable or "nearly" stable if $f(r_1,..,r_N; \theta_1,..,\theta_N)$ is a local minimum or a saddle point at these coordinates. In either case the pattern is stationary in the rotating frame. Beginning with an arbitrary configuration of vortices, an obvious way to find minima is to move the vortices successively toward lower energy configurations until a minimum is reached. The pattern may pass through one or more saddle points before it converges to a local minimum in the free energy. A simple algorithm to accomplish this consists of assigning to each vortex an effective velocity $\underset{\sim}{u}_j$ equal to the negative gradient of the free energy with respect to the coordinates of that vortex, $-\underset{\sim}{\nabla}_j f$. Allowing

the vortices to move in steps proportional to this effective velocity, which changes after each step, results in a convergent pattern. This procedure works well except for angular velocities less than a critical value $\omega^*(N)$ for which no free energy minima exist. For $N \leq 20$ we find $\omega^*(N) \approx N \div 2$.

In deriving the velocity expression it is convenient to use complex numbers, $z = x + iy$, $\bar{z} = x - iy$, which allows the free energy to be written as

$$f = \ell n \left[\frac{\prod_i (1-|z_i|^2) \prod_{i<j} |1-z_i\bar{z}_j|^2}{\prod_{i<j} |z_i - z_j|^2} \right] - \omega \sum_i (1-|z_i|^2) + N \ell n (R/a) \quad . \tag{2}$$

The gradient transforms to complex notation as $\nabla_j f \to 2 \frac{\partial}{\partial \bar{z}} f$ which gives the following expression for the pattern-converging velocity of the j^{th} vortex,

$$\tfrac{1}{2}(u_{jx} + i u_{jy}) = \sum_{\ell}{}' \frac{1}{\bar{z}_j - \bar{z}_\ell} - \sum_{\ell} \frac{1}{\bar{z}_j - 1/z_\ell} - \omega z_j \quad , \tag{3}$$

where the prime on the first summation indicates that $\ell \neq j$. The first summation represents the influence of all the image vortices and the second summation gives the effect of all the other vortices on the j^{th}. This velocity field is exactly orthogonal to the velocity field v in the rotating frame of a classical hydrodynamic vortex system which causes the vortices to move physically on an equipotential surface of $f(z_i)$: $u \propto - iv$. To see this, recall that the velocity of a classical vortex is the stream velocity at its position. In dimensional units, v is given by the derivative of the stream function

$$\overline{V(Z)} = - \frac{\partial}{\partial Z} W(Z) \quad , \tag{4}$$

which, for identical vortices inside a circular cylinder, is[4]

$$W(Z) = i \frac{\kappa}{2\pi} \left[\sum_{\ell=1}^{N} \ell n (Z - Z_\ell) - \sum_{\ell=1}^{N} \ell n (R^2 - Z\bar{Z}_\ell) \right] . \tag{5}$$

To use a reference frame in which the boundary is at rest requires the addition to W(Z) of the stream function for solid body rotation in the direction

opposite to the laboratory rotation - $i\Omega|Z|^2$, where Ω is the physical value of the angular velocity. The physical stream velocity at Z is, therefore,

$$\overline{v(Z)} = -\frac{\partial}{\partial Z}\left[W(Z) - i\Omega|Z|^2\right] , \tag{6}$$

which becomes, upon defining $z \equiv Z/R$ and $\omega \equiv 2\pi R^2\Omega/\kappa$,

$$\frac{2\pi R}{\kappa}\,\overline{v(z)} = -i\left[\sum_{\ell}\frac{1}{z-z_\ell} - \sum_{\ell}\frac{1}{z-1/\bar{z}_\ell} - \omega\bar{z}\right]. \tag{7}$$

Taking the conjugate of the above equation and comparing with Eq. (3) confirms that $u(z) \propto - iv(z)$. (When $z = z_j$, the $j = \ell$ term must be omitted in the first summation in Eq. (7) because a vortex does not contribute directly to its own velocity.) Any system of vortices whose motion follows only the classical velocity of Eq. (7) can never converge to a stationary pattern in the rotating frame for the obvious reason that such motion is constrained to an equipotential surface of the free energy. However, the physical velocity w of superfluid vortices has components parallel to both v of Eq. (7) and u of Eq. (3), the latter component arising from irreversible frictional dissipation that accompanies all relative motion between superfluid vortices and the normal component of superfluid helium. That is,

$$w = (d_1 - id_2)v ,$$

where the relative magnitude of the positve real coefficients d_1 and d_2 depends on the temperature and the concentration of ^{3}He impurities. (Because of the quantum nature of the superfluid state, the integrity of the circulation of the vortices is unaffected by the above frictional effects.) Although there are no physical conditions for which $d_1/d_2 = 0$, we have no reason to expect that any stationary patterns calculated by an algorithm that assumes $d_1/d_2 = 0$ are inaccessible to the physical system for that reason.

We find that the N and ω dependences of the free energy of stationary patterns as given by Eq. (1) or (2) can be expressed to good accuracy by a relatively simple analytic formula, namely, the free energy f_c of a "continuum" consisting of vortices in a perfect triangular lattice (see Eq. (1) of Ref. 3),

$$f_c(N,\omega) = \tfrac{1}{2} N^2 \left(\frac{3}{2} - \ell n\ N\right) - \omega N + \tfrac{1}{2} N(N-1)\ell n\ \omega$$

$$-Nb + N\ \ell n\ R/a\ , \qquad (8)$$

where $b = 4.15041281/\pi - \ell n\ \sqrt{\pi} = 0.748752485$. Using Eq. (8) we are able to express the free energies of patterns as a small difference $\Delta f(N,\omega) \equiv f - f_c$. Moreover, <u>$\Delta f$ is an insensitive function of the angular velocity</u> if the latter is not near the critical value ω^*; when ω increases, Δf quickly reaches an asymptotic value characteristic of the given stationary pattern. Therefore, we may simply and uniquely specify a Δf_0 for each pattern by defining

$$\Delta f_0(N) \equiv \lim_{\omega\to\infty} \Delta f(N,\omega).$$

This asymptotic value for large ω is equivalent to ignoring the effects of images in the calculation of f at <u>any</u> positive ω. (For ω somewhat smaller than $\omega^*(N)$ the radius of the vortex pattern will exceed the radius of the container, $r = 1$; this is formally permissible in the absence of images.) A considerable saving of computation is thereby realized both in the calculation of the vortex velocities (the image sum in Eq. (3) can be omitted) and in the calculation of Δf. To derive the simplified form of Δf, substitute $r_j' \sqrt{\omega'/\omega}$ for r_j in Eq. (1) (because the radii scale as $\sqrt{\omega}\ r_j = \sqrt{\omega'}\, r_j'$ for moderately large ω) and take the limit as $\omega\to\infty$. This gives, after omitting the primes on r_j for notational convenience,

$$\lim_{\omega\to\infty} f = -\ell n \prod_j \prod_{i<j} (r_i^2 + r_j^2 - 2r_i r_j \cos\theta_{ij})$$

$$+ \tfrac{1}{2} N(N-1)\ell n\omega/\omega' - N\omega + \omega' \Sigma\, r_j^2 + N\ \ell n\ R/a\ . \qquad (9)$$

Therefore, using Eq. (8),

$$\Delta f_o \equiv \lim_{\omega \to \infty} f - f_c = -\ln \prod_{j<i} \left(r_i^2 + r_i^2 - 2r_i r_j \cos\theta_{ij}\right) + \omega' \Sigma\, r_j^2$$

$$-\tfrac{1}{2} N^2 \left(\tfrac{3}{2} - \ln N\right) - \tfrac{1}{2} N(N-1) \ln \omega' + Nb \,, \tag{10}$$

where the positions $\underset{\sim}{r}_j$ are calculated for the positive, but otherwise arbitrary, angular velocity ω'.

The behavior of $\Delta f(N,\omega)$ and the scaling of $\sqrt{\omega} r$ as functions of ω are illustrated in Table I for N = 18. Here $r_{18}(18_1)$ is the radius of the outermost vortex in the first (i.e., lowest energy) pattern of 18 vortices. The pattern 18_1 became unstable for $\omega \approx 19.9$, somewhat lower than for the pattern 18_7 . Already at $\omega = 25$, Δf is within 3% of its value at $\omega = \infty$. This relative insensitivity of Δf on ω is emphasized in the fourth column. As might be expected, the free energy difference between patterns is even less sensitive to ω; this is illustrated in the fifth column for patterns 18_1 and 18_7.

The patterns were calculated by letting an initial vortex configuration develop in "time" steps Δt according to Eq. (3) until Δf_o reached a constant value within 10^{-5}. The positions of all vortices were changed simultaneously at each Δt step where $\Delta t \approx 0.2/(\omega - N)$ was used.

We began each pattern calculation with an initial configuration of rings of vortices, centered about the origin, at radii roughly consistent with the value of ω used. (We found that patterns of higher free energy were not produced efficiently when random arrays were used as the initial configuration.) The resulting convergent pattern was then compared with patterns previously obtained for the same N and ω and, if different, was saved.

TABLE I

VARIATION OF PATTERN FREE ENERGY AND SIZE WITH ANGULAR VELOCITY

ω	$\Delta f(18_1)$	$\sqrt{\omega}\, r_{18}(18_1)$	$\Delta f_0 - \Delta f(18_1)$	$\Delta f(18_7) - \Delta f(18_1)$
∞	0.25241[a]	3.515846	0	0.22487
90	0.25241	3.515859	-0.00000	0.22487
80	0.25240	3.515868	-0.00001	0.22486
70	0.25240	3.515890	-0.00001	0.22486
60	0.25238	3.515943	-0.00003	0.22485
50	0.25232	3.516094	-0.00009	0.22482
40	0.25211	3.516637	-0.00030	0.22474
30	0.25068	3.519597	-0.00173	0.22447
25	0.24539	3.527177	-0.05301	0.22463
20[c]	0.18940	3.612616	-0.06301	...[b]

[a] $f_0(18_1)$.

[b] Pattern 18_7 diverged for $\omega = 20$.

[c] $\omega^*(18_1) \approx 19.9$.

III. PATTERN SUMMARY

In Table II are listed the free energies Δf_0 and ring numbers of the patterns. The ring numbers are the number of vortices with radii that differ by less than 0.02 (except for $N > 50$ where the criterion is 0.05). For example, 14 vortices form a pattern that is roughly (within 0.02) a ring of 4 inside a ring of 10, making the ring number of this pattern (4, 10).

In principle, Table II can be used to find the net free energy of a specific pattern. Given the experimental conditions of cylinder radius R and angular velocity Ω, one merely adds Δf_0 of Table II to f_c as calculated

according to Eq. (8). (As shown in Table I, some accuracy will be lost if ω is near ω^*.) For example, if R = 0.5 cm and $\Omega = 2\pi/60\ s^{-1}$ (that is, 1 rpm) then $\omega = 164.4934$ and, except for temperatures near the superfluid transition, $R/a = 3.6\ 10^7$. From Eq. (8), a continuum pattern of 5 vortices would have (dimensionless) free energy $f_c = -689.5549$, so the net energies of the discrete patterns are $f(5_1) \approx f_c + \Delta f_0(5_1) = -689.4218$ and $f(5_2) \approx -689.1512$. However, to calculate f_c to an accuracy of only 0.1, comparable to the larger differences between Δf_0 of the various patterns for a given N, one must know R/a and Ω to unrealistically high accuracy. In this example, the necessary accuracy is 0.02% for R/a and 0.01% for Ω. Consequertly, the Δf_0 of Table II, like other fine structure energies, are more relevant to experiments of high relative precision than those of absolute accuracy.

If, for given experimental conditions, it is a question of which of all patterns has the lowest free energy, one must first find N by minimizing $f_c(N,\omega)$ with respect to N. This results in a transcendental equation,

$$0 = N \ln N - N(1 + \ln \omega) + \omega + 1/2 \ln\omega + b - \ln R/a \qquad (11)$$

which can be formally solved for N by iteration if ω lies between the two limits, $\omega_1 < \omega < \omega_2$, where

$$\omega_1 + 1/2 \ln\omega_1 = \ln R/a - b \qquad (12.1)$$

and

$$\omega_2 = \left(\frac{R}{a}\right)^2 e^{-2b} . \qquad (12.2)$$

The first limit requires a minimum angular velocity for any vorticity and the second limit prevents vortex densities so large that the vortex cores overlap. For the example used above, $\omega_1 = 15.3$, $\omega_2 = 2.85\ 10^{14}$, and the minimum in f_c occurs for N = 103. The free energy f_c for this optimum number of vortices differs appreciably from that (f_s) for solid-body rotation, $(f_s - f_c)/f_s = 0.25$, which shows that quantum effects are still important in patterns of 100 vortices. (For ω 10 times larger, the optimum vortex number is 16 times greater and the above ratio is reduced to 0.03.)

TABLE II

FREE ENERGIES AND RING NUMBERS OF KNOWN

STABLE VORTEX PATTERNS

N	Order	Δf_0	Ring Numbers
1	1	-.00125	1
2	1	.19065	2
3	1	.14418	3
4	1	.10740	4
5	1	.13307	5
	2	.40365	1, 4
6	1	.21781	1, 5
	2	.24927	6
7	1	.10749	1, 6
8	1	.09454	1, 7
9	1	.19405	1, 8
	2	.26694	2, 4, 3
	3X[a]	.26716	2, 3, 4
	4X	.54366	3, 6,
10	1	.22433	2, 4, 4
	2	.22578	2, 2, 4, 2
	3	.41705	1, 9
11	1	.24918	3, 8
	2	.28859	2, 9
12	1	.19344	3, 3, 6
	2X	.19837	3, 6, 3
	3	.35022	4, 8
13	1	.22432	4, 9
	2	.24636	3, 10
14	1	.17790	4, 10
	2	.36713	5, 9
15	1	.23413	4, 11
	2	.24711	5, 10
	3	.24773	5, 10

16	1	.21959	5, 11
	2	.36491	1, 5, 10
	3X	.38647	1, 5, 5, 5
	4	.39842	4, 4, 8
	5	.40541	4, 8, 4
17	1	.28394	1, 5, 11
	2	.29412	5, 12
	3	.34894	3, 3, 11
	4	.39682	1, 6, 10
	5	.47407	1, 4, 4, 8
18	1	.25241	1, 6, 11
	2	.28316	1, 5, 12
	3	.35110	3, 3, 12
	4	.35215	6, 12
	5	.35241	3, 3, 12
	6	.35626	6, 12
	7	.47728	5, 13
19	1	.18626	1, 6, 6, 6
	2	.19317	1, 6, 12
	3	.33323	1, 7, 11
	4	.38032	1, 5, 13
	5	.45481	3, 3, 13
20	1	.21955	1, 6, 13
	2	.21960	1, 7, 12
	3X	.43685	2, 2, 4, 12
	4X	.46897	2, 4, 2, 6, 4, 2
21	1	.19096	1, 7, 13
	2	.34793	1, 6, 6, 8
	3	.37628	1, 4, 4, 12
	4	.39590	2, 2, 2, 3, 12
22	1	.25122	1, 7, 7, /
	2X	.26311	1, 7, 14
	3	.30426	1, 8, 13
	4	.33339	2, 7, 13
23	1	.31390	1, 8, 14
	2	.33704	2, 2, 4, 2, 13
	3	.33801	2, 2, 2, 3, 14
	4	.42158	1, 7, 15
24	1	.30037	2, 2, 4, 2, 14
	2	.39788	3, 8, 13
	3	.41961	1, 8, 15
	4	.44624	1, 1, 2, 2, 3, 15
	5	.44889	2, 2, 2, 4, 1, 13

25	1	.32980	3, 8, 14
	2	.35268	2, 2, 4, 2, 15
	3	.35301	2, 2, 4, 2, 15
	4	.37705	2, 2, 7, 14
	5	.42524	2, 1, 3, 6, 13
	6	.61199	1, 8, 8, 8
26	1	.31762	3, 3, 6, 14
	2	.33269	3, 8, 15
	3	.38172	2, 1, 2, 6, 15
	4	.48666	2, 2, 4, 2, 8, 8
27	1	.27672	3, 3, 6, 15
	2	.38716	4, 9, 14
	3	.40983	3, 8, 16
	4	.41204	3, 4, 6, 14
	5X	.43807	3, 8, 16
	6	.47419	2, 1, 2, 6, 16
28	1	.32073	4, 9, 15
	2	.32482	3, 3, 6, 16
	3	.34232	3, 5, 5, 15
	4	.34311	3, 10, 15
	5	.40699	4, 4, 6, 14
	6	.43942	4, 8, 8, 8
	7X	1.34475	1, 9, 18
29	1	.31163	4, 10, 15
	2	.32340	4, 9, 16
	3	.34598	3, 3, 7, 16
	4	.45988	3, 3, 6, 17
30	1	.27672	4, 4, 6, 16
	2	.39429	4, 11, 15
	3	.40588	5, 5, 5, 15
	4	.40738	4, 9, 17
	5	.43543	3, 3, 7, 17
37	1	.28424	1, 6, 6, 6, 18
	2	.28884	1, 6, 6, 6, 18
	3	.39854	1, 7, 12, 17
	4	.41983	1, 6, 11, 19
50	1	.44156	4, 10, 15, 21
	2	.45244	4, 9, 16, 21
	3	.46482	3, 3, 6, 16, 22
	4	.48020	3, 3, 7, 15, 22
	5	.49186	4, 4, 6, 16, 20
	6	.54319	3, 3, 6, 9, 6, 23
	7	.62067	3, 2, 2, 6, 17, 20

61	1	.39758	1, 6, 12, 18, 24
	2	.42173	1, 6, 12, 18, 24
91	1	.53680	1, 6, 12, 18, 24, 30
	2	.58631	1, 6, 12, 18, 24, 30
127	1	.70345	1, 6, 12, 18, 24, 30, 36
	2	.73294	1, 6, 12, 18, 24, 30, 36
169	1	.89830	1, 6, 12, 18, 24, 30, 36, 42
	2	1.01167	1, 6, 12, 18, 24, 30, 36, 42
217	1	1.12214	1, 6, 12, 18, 24, 30, 36, 42, 48
	2	1.27248	1, 6, 12, 18, 24, 30, 36, 42, 48

[a] X denotes patterns that are nearly stable.

As N increases, the pattern with lowest energy changes from 1 vortex in the center to 2, 3, 4, 5, and then back to 1 (N = 6), 2 (N = 10), 3, 4, 5, and again, 1 (N = 17). Having 1 vortex in the center of the lowest energy pattern is a property of vortex numbers close to "triangular" ring numbers N = 1 + 6 (1 + 2 + 3 + ...), that is, N = 1, 7, 19, 37, 61, 91, 127, 169, 217, etc.

IV. PATTERN FIGURES

The patterns are illustrated in the Catalog below in order of increasing vortex number N and, for each N, in order of increasing Δf_0, which is the asymptotic free energy difference with respect to the continuum model as $\omega \to \infty$. We show all the stable patterns we have found for $N \leq 30$ and N = 37, 50. (Patterns 37_2 and 37_3 were shown by Stauffer and Fetter.[3]) In addition we include a few of the many nearly stable patterns, which are identified by an "X" in the upper right-hand corner. For N = 61, 91, 127, 169, 217 only the two lowest energy patterns are shown.

In addition to Δf_0, the ring numbers (defined in Sec. III) are also listed below each pattern. A result of the fine discrimination applied to patterns with $N \leq 50$ is ring numbers that are, in several cases, expanded beyond what one sees by cursory inspection. For instance, pattern 9_2 has ring numbers (2, 4, 3) although on a coarser scale they would obviously be (2, 7). The 2% criterion permits unique ring numbers to most patterns that are similar, such as 9_2 and 9_3, but still not all, such as 15_2 and 15_3.

As explained in Sec. II, the absence of image effects makes Δf_0 independent of the value of angular velocity ω used to calculate the pattern. The pattern size, however, does depend on ω and an accurate estimate of the radii of the various rings constituting a pattern can be derived from the exact second-moment relation that every stationary (stable or nearly stable) pattern in an unbounded fluid must satisfy[5]:

$$\omega \sum_{j=1}^{N} r_j^2 = \tfrac{1}{2} N(N-1) \ . \tag{13}$$

Assuming the pattern consists of M rings of radii $r_1,..,r_M$, each containing $N_1,..,N_M$ vortices, respectively, the ring radii satisfy

$$\omega\, r_j^2 = \tfrac{1}{2}(N_j-1) + N_1 + N_2 + .. + N_{j-1}, \qquad 1 \leq j \leq N \ . \tag{14}$$

This formula is most useful for rings that do not deviate appreciably from circles. In Table III are listed the values of ω used here.

TABLE III

ANGULAR VELOCITY USED IN PATTERN CALCULATIONS

N	ω
1 through 15	N + 10
16 through 30	N + 8
37	50
50	65
61	80
91	125
127	185
169	250
217	330

The patterns for N = 61, 91, 127, 169, 217 are included to illustrate the tendencies of those patterns which most closely approximate triangular symmetry which is known to be the preferred pattern for an infinite number of vortices. However, for each of these N, the pattern N_1 of lowest free energy has less triangular symmetry than N_2. In addition, the triangular lattices of both N_1 and N_2 suffer circular distortion that penetrates deeply into the patterns. (This is most easily seen by looking obliquely at the figures.) Because these patterns are calculated in the absence of images they show that a finite pattern of vortices, even in an infinite container, displays triangular symmetry in less than half of its total area. This circular distortion results in a free energy that is greater than the (continuum model) value for an equal number of vortices in an infinite and perfect triangular lattice. This additional energy per vortex appears to be approaching a limiting value as N increases: $\Delta f_0(N)/N$ = 0.00590, 0.00554, 0.00532, 0.00517 for N = 91, 127, 169, and 217, respectively. For comparison, the extra energy per vortex in a perfect square lattice is 0.01058. Although the deviation Δf_0 of the free energy with respect to the continuum model increases with larger N, the ratio of this deviation to the total free energy decreases rapidly.

The nearly stable patterns are shown here to serve as a cautionary sample of patterns that may initially show excellent convergence, both spatially and in their second moment, Eq. (13), but are not subsequently stable. This is especially true of many patterns derived from initial vortex configurations of high symmetry such as those having ring numbers (m, 2m) or (m, 3m) or (1, m, 2m), etc. The free energy of these patterns is at a saddle-point and continued numerical iteration of the pattern around the apparent stable configuration will lead to the injection, through computer round-off error, of finite amplitude into the unstable modes of the pattern which then grow, leading to a new stable (or perhaps nearly stable) pattern. The acquisition of nearly stable patterns can be largely avoided by slightly randomizing the initial configuration.

CATALOG OF VORTEX
PATTERNS

1_1

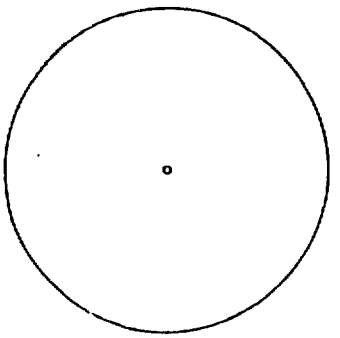

-.0012
1

2_1

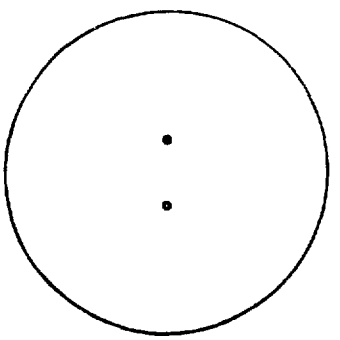

.1906
2

3_1

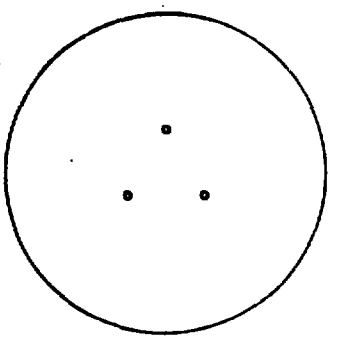

.1442
3

4_1

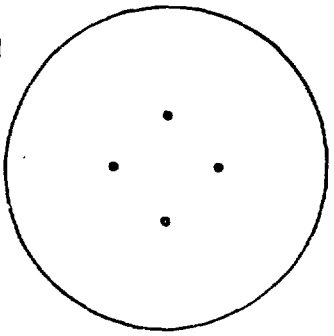

.1074

4

5_1

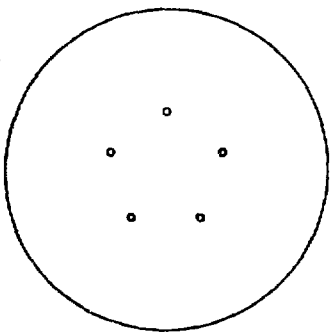

.1331

5

5_2

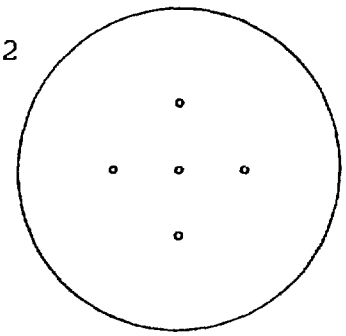

.4037

1 4

6_1

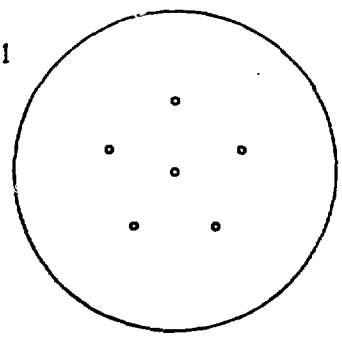

.2178

1 5

6_2

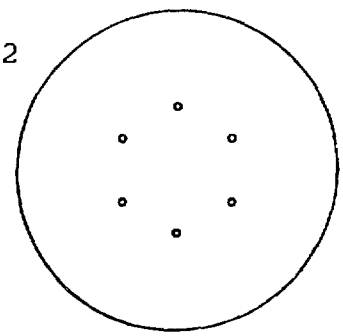

.2493

6

7_1

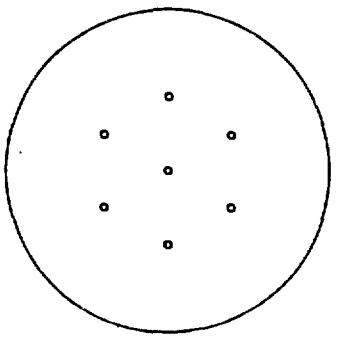

.1075

1 6

8_1

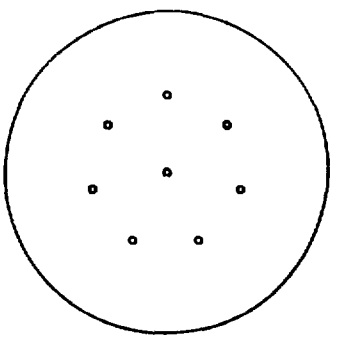

.0945

1 7

9_1

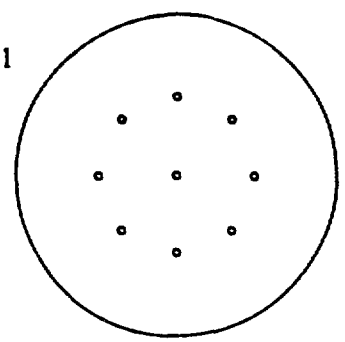

.1940

1 8

9_2

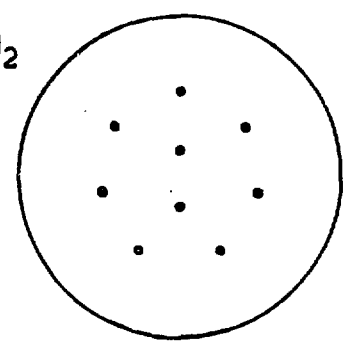

.2669

2 4 3

9_3 x

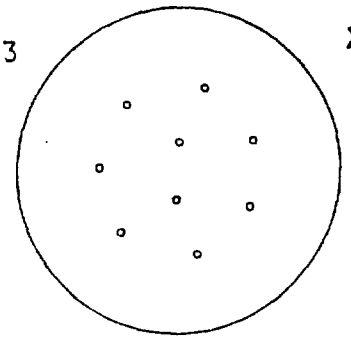

.2672

2 3 4

9_4 x

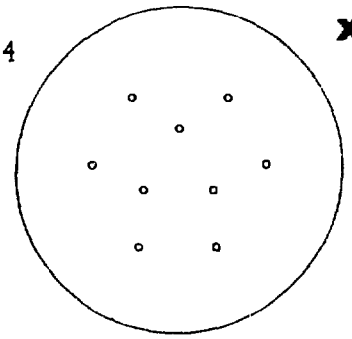

.5437

3 6

10_1

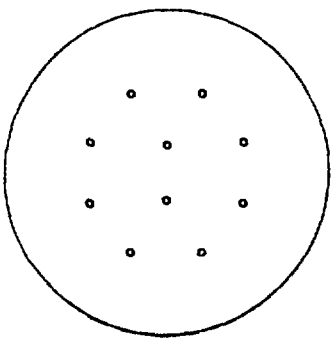

.2243

2 4 4

10_2

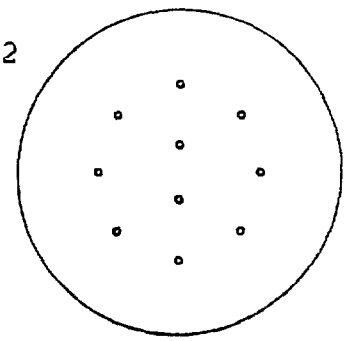

.2258

2 2 4 2

10_3

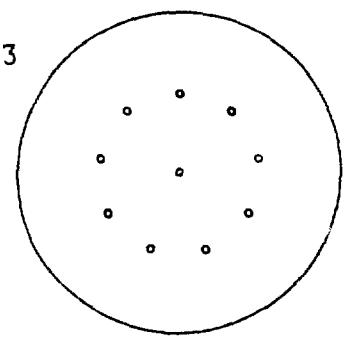

.4170

1 9

11_1

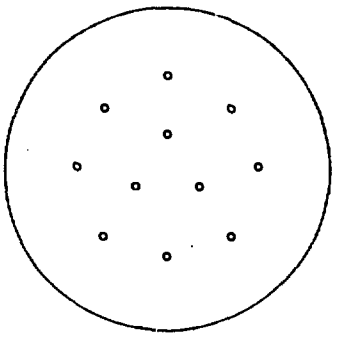

.2492

3 8

11_2

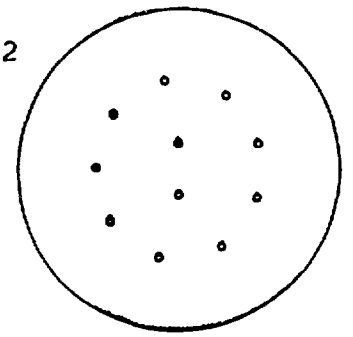

.2886

2 9

12_1

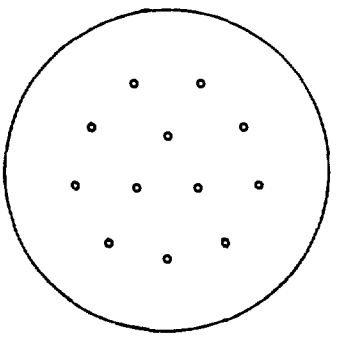

.1934

3 3 6

12_2 **x**

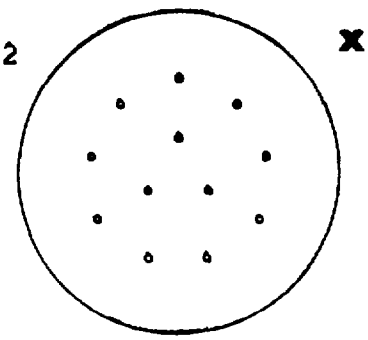

.1984

3 6 3

12_3

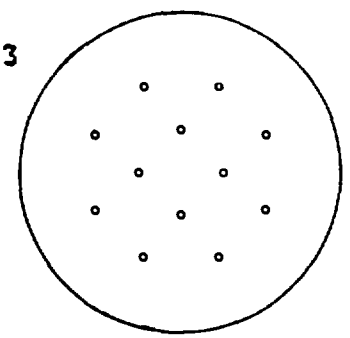

.3502

4 8

13_1

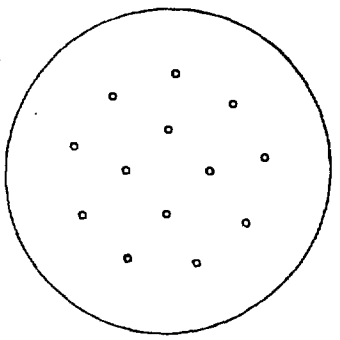

.2243

4 9

13_2

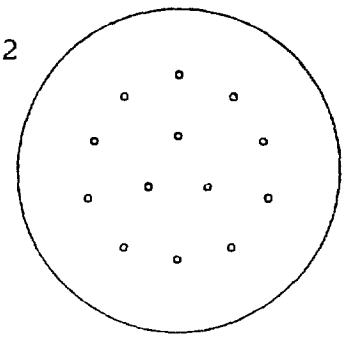

.2464

3 10

14_1

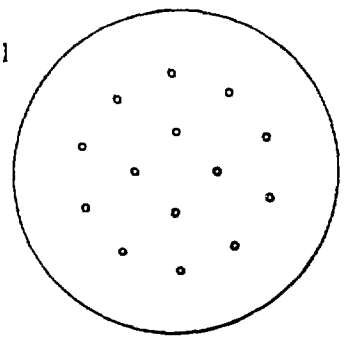

.1779

4 10

14_2

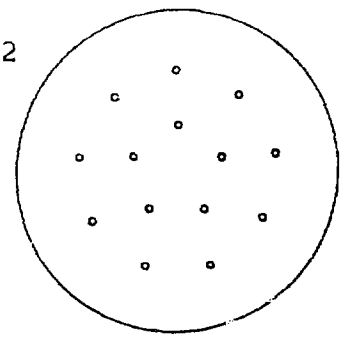

.3671

5 9

15_1

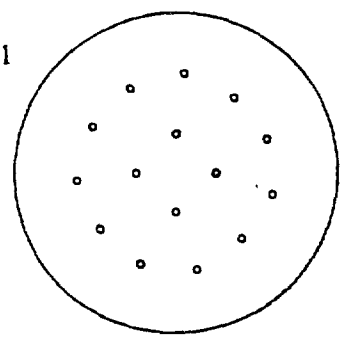

.2341

4 11

15_2

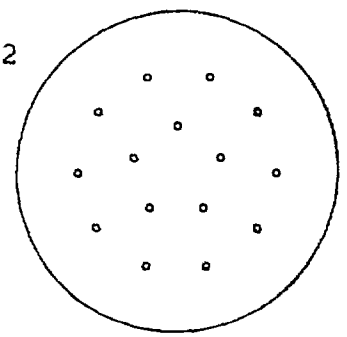

.2471

5 10

15_3

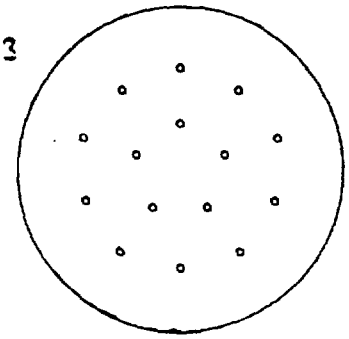

.2477

5 10

16_1

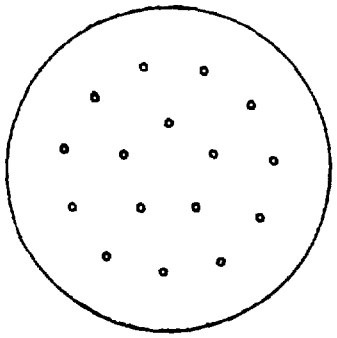

.2196

5 11

16_2

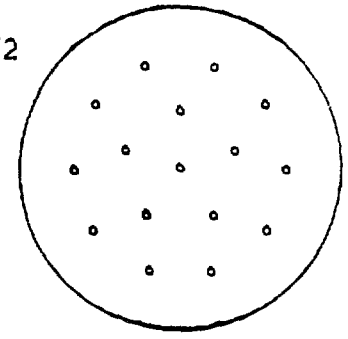

.3649

1 5 10

16_3 x

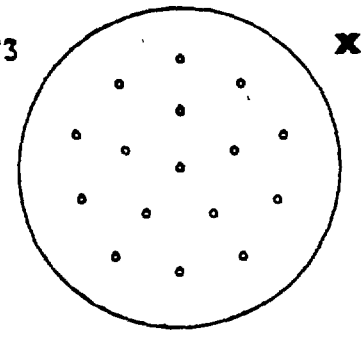

.3865

1 5 5 5

16_4

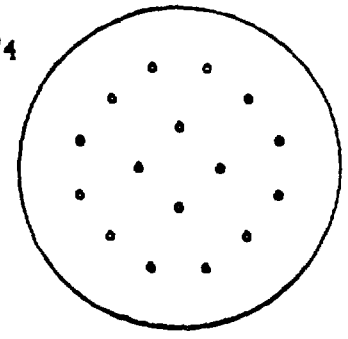

.3984

4 4 8

16_5

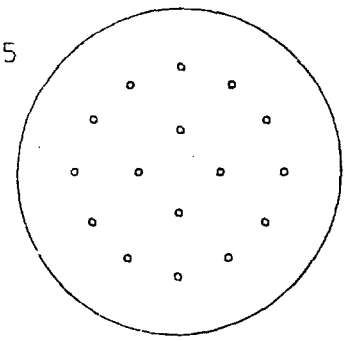

.4054

4 8 4

17_1

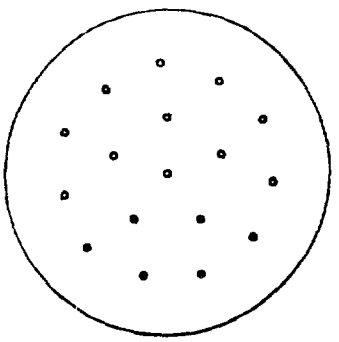

.2839

1 5 11

17_2

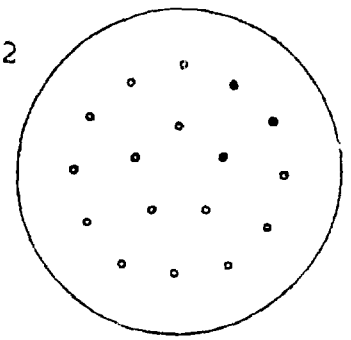

.2941

5 12

17_3

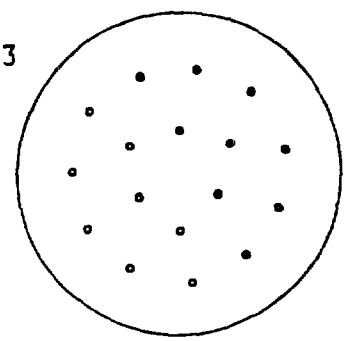

.3489

3 3 11

17_4

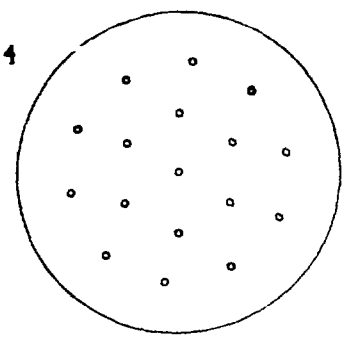

.3968

1 6 10

17_5

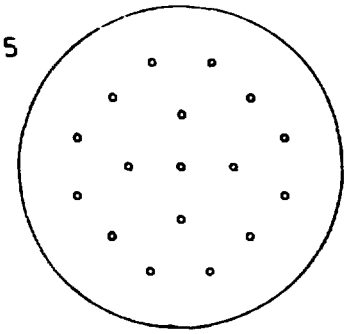

.4741

1 4 4 8

18_1

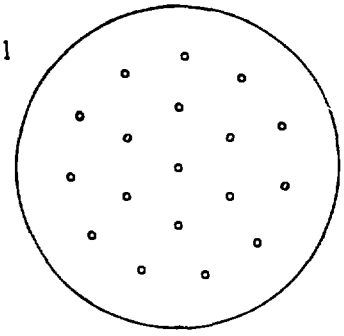

.2524

1 6 11

18_2

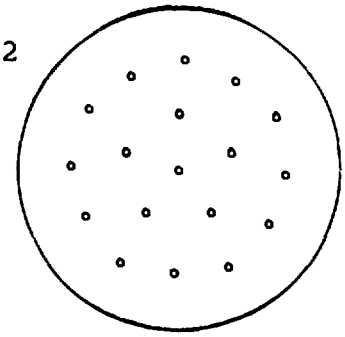

.2832

1 5 12

18_3

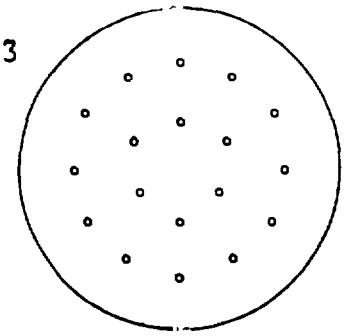

.3511

3 3 12

18_4

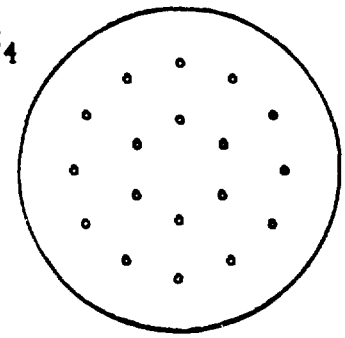

.3521

6 12

18_5

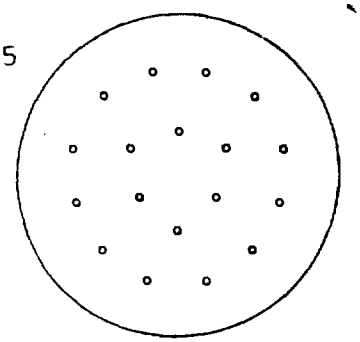

.3524

3 3 12

18_6

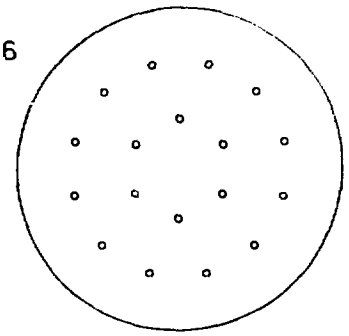

.3563

6 12

18_7

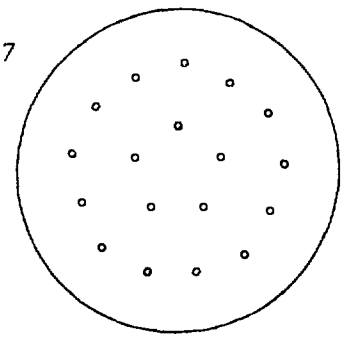

.4773

5 13

19_1

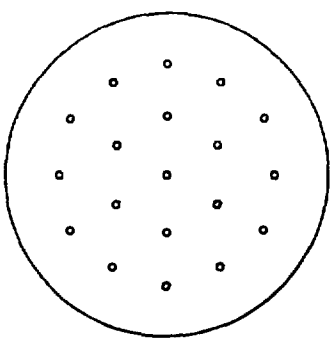

.1863

1 6 6 6

19_2

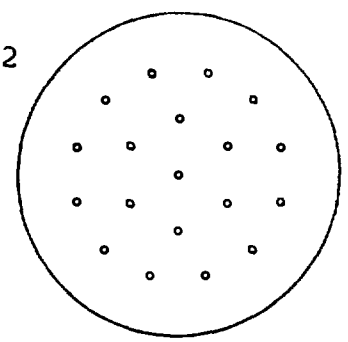

.1932

1 6 12

19_3

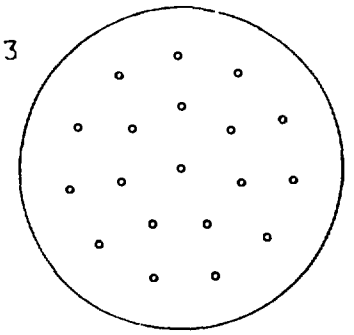

.3332

1 7 11

19_4

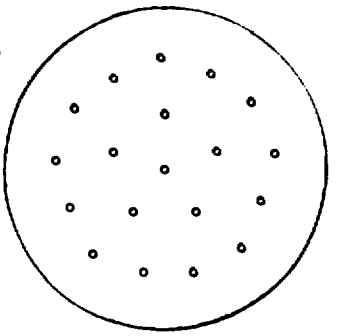

.3803

1 5 13

19_5

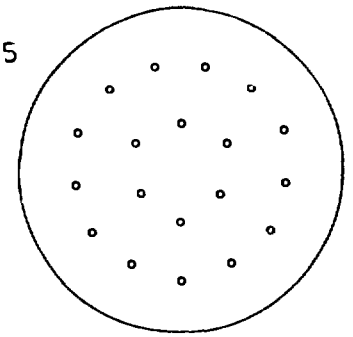

.4548

3 3 13

20_1

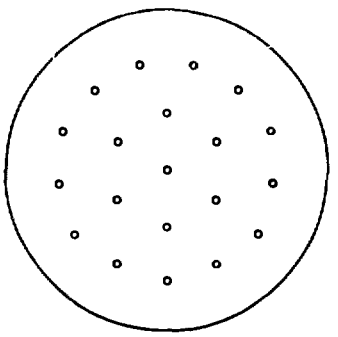

.2195

1 6 13

20_2

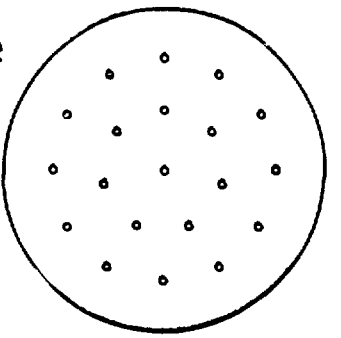

.2196

1 7 12

20_3 x

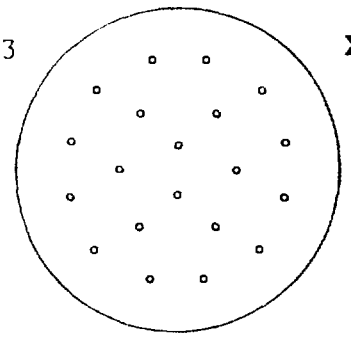

.4368

2 2 4 12

20_4 x

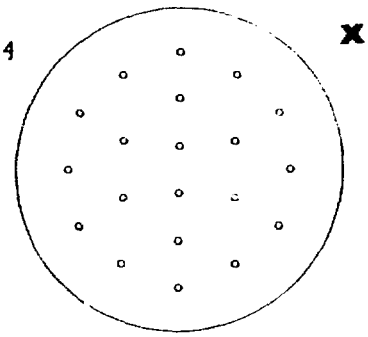

.4690

2 4 2 6 4 2

21_1

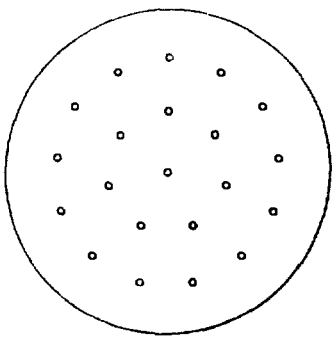

.1910

1 7 13

21_2

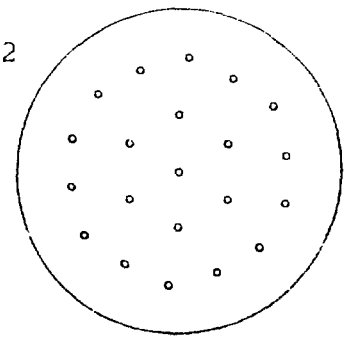

.3479

1 6 6 8

21_3

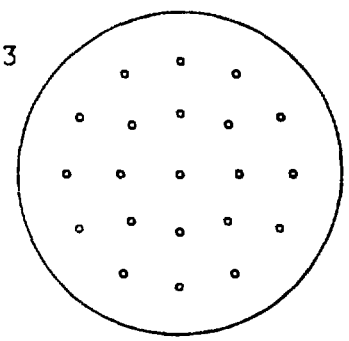

.3763

1 4 4 12

21_4

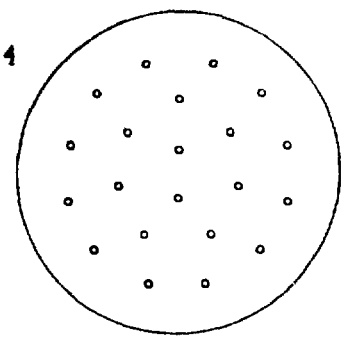

.3959

2 2 2 3 12

22_1

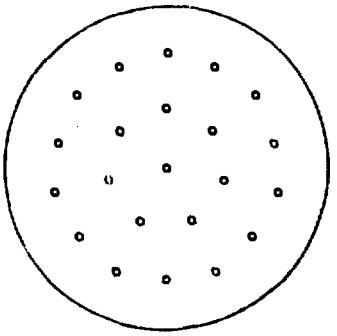

.2512

1 7 7 7

22_2 ✖

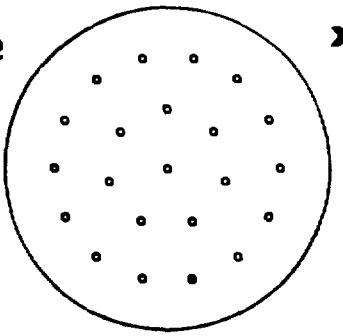

.2631

1 7 14

22_3

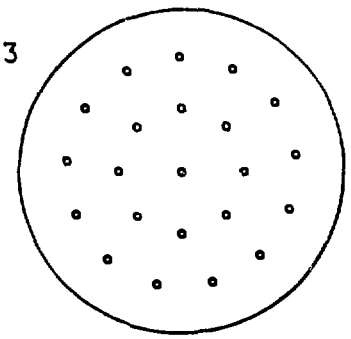

.3043

1 8 13

22_4

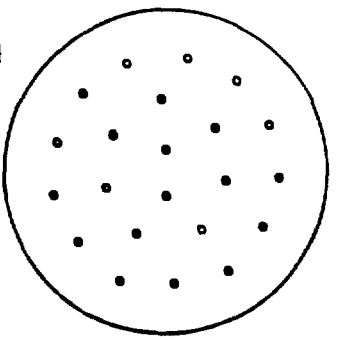

.3334

2 7 13

23_1

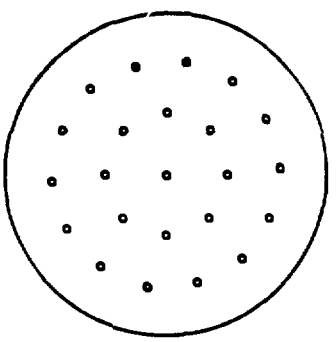

.3139

1 8 14

23_2

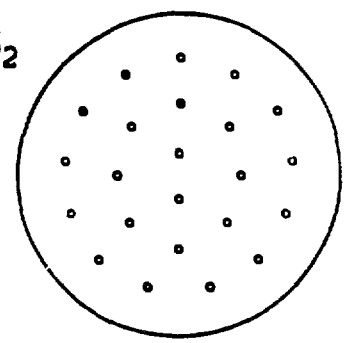

.3370

2 2 4 2 13

23_3

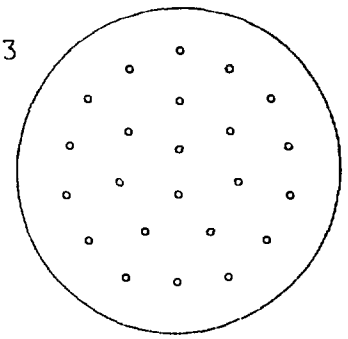

.3380

2 2 2 3 14

23_4

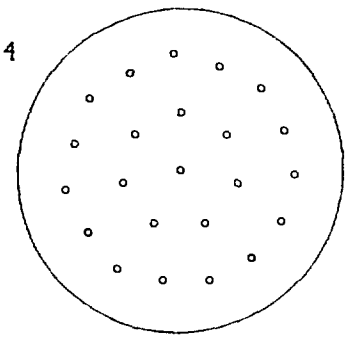

.4216

1 7 15

24_1

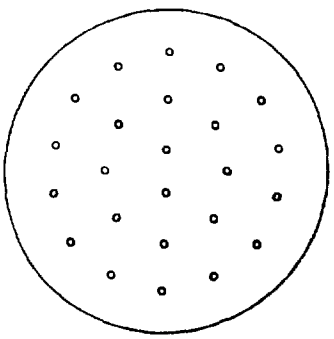

.3004

2 2 4 2 14

24_2

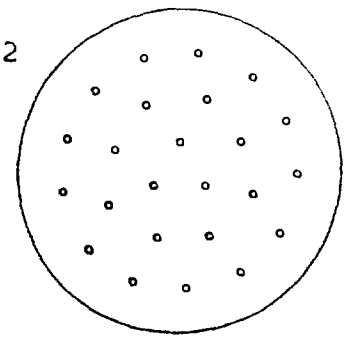

.3979

3 8 13

24_3

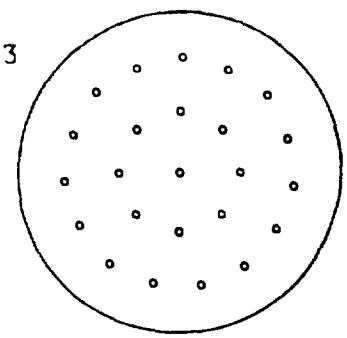

.4196

1 8 15

24_4

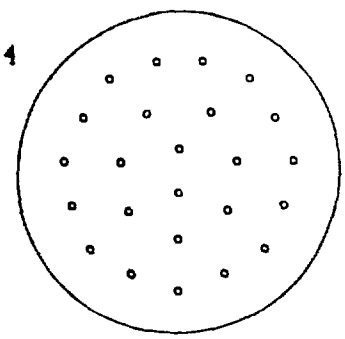

.4462

1 1 2 2 3 15

24_5

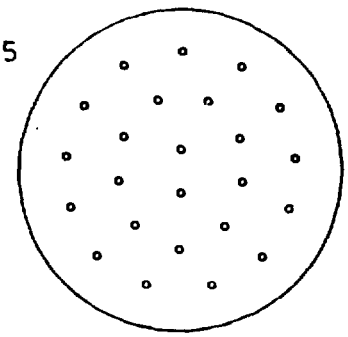

.4489

2 2 2 4 1 13

25_1

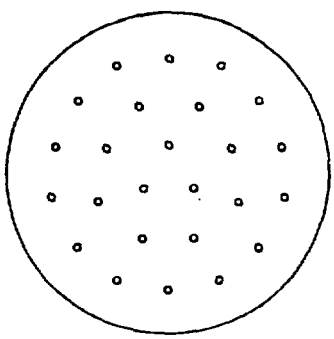

.3298

3 8 14

25_2

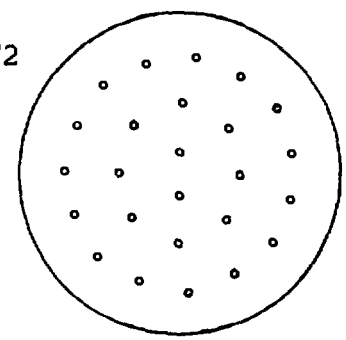

.3527

2 2 4 2 15

25_3

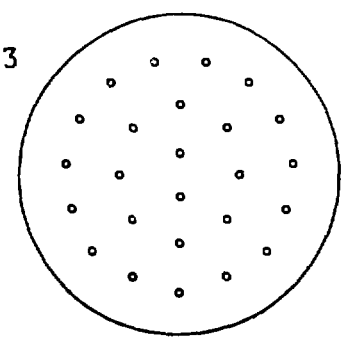

.3530

2 2 4 2 15

25_4

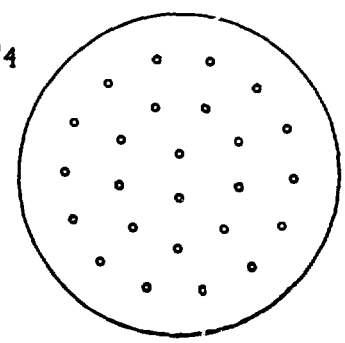

.3771

2 2 7 14

25_5

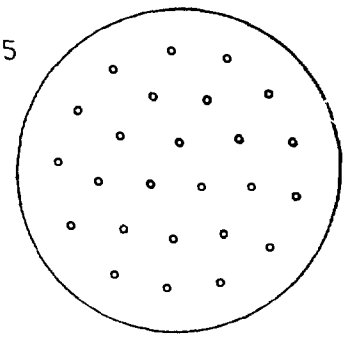

.4252

2 1 3 6 13

25_6

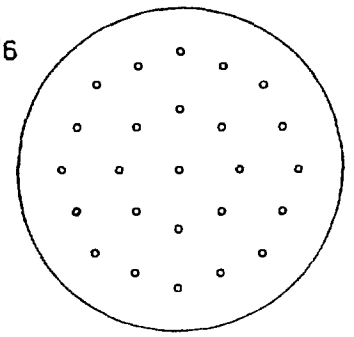

.6120

1 8 8 8

26_1

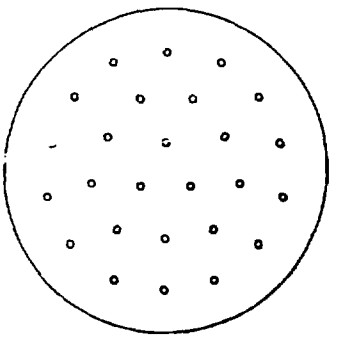

.3176

3 3 6 14

26_2

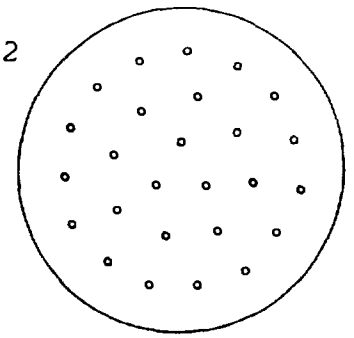

.3327

3 8 15

26_3

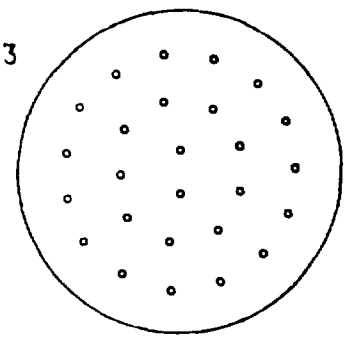

.3817

2 1 2 6 15

26_4

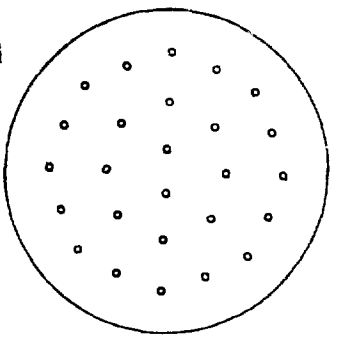

.4867

2 2 4 2 8 8

27_1

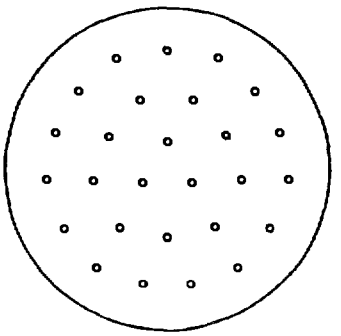

.2767

3 3 6 15

27_2

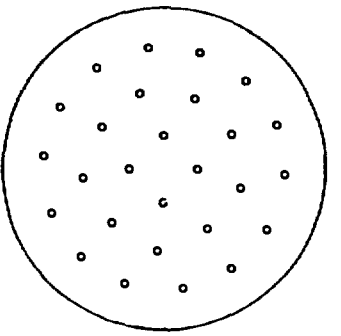

.3872

4 9 14

27_3

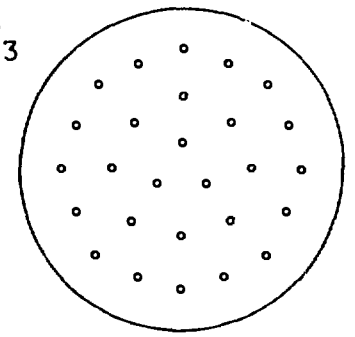

.4098

3 8 16

27_4

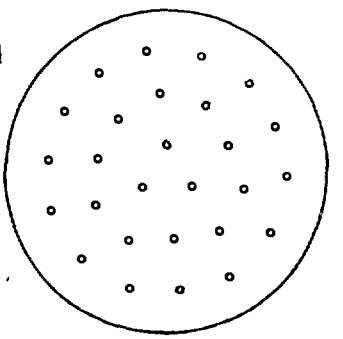

.4120

3 4 6 14

27_5 ✖

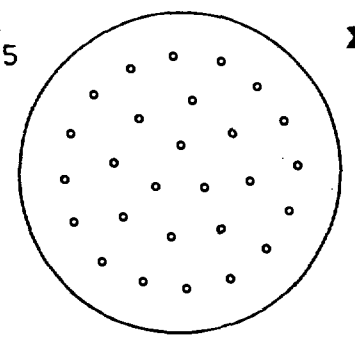

.4381

3 8 16

27_6

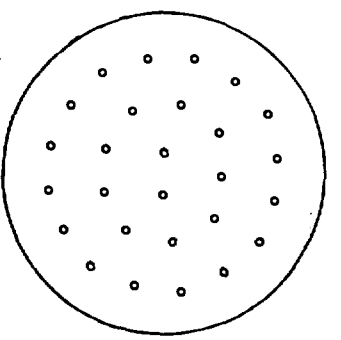

.4742

2 1 2 6 16

28_1

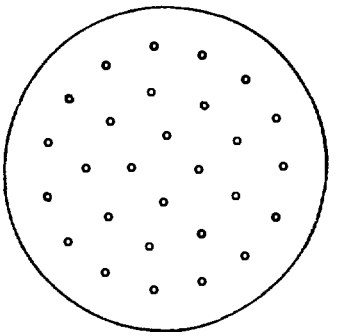

.3207

4 9 15

28_2

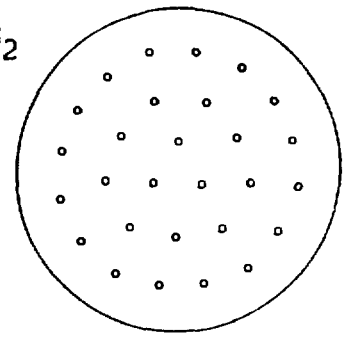

.3248

3 3 6 16

28_3

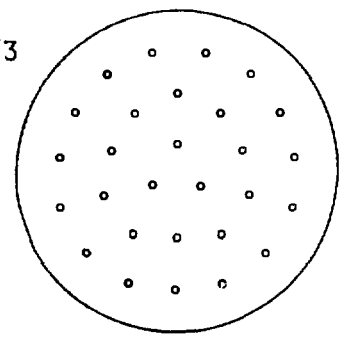

.3423

3 5 5 15

28_4

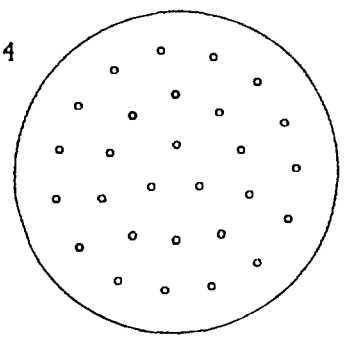

.3431

3 10 15

28_5

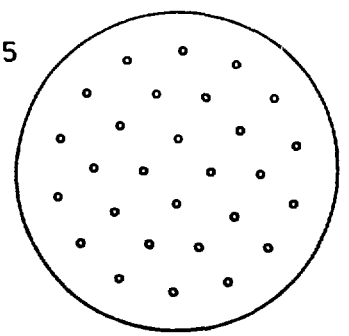

.4070

4 4 6 14

28_6

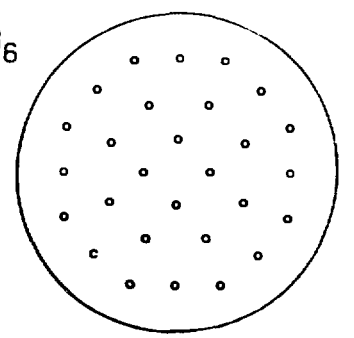

.4394

4 8 8 8

28_7 ✖

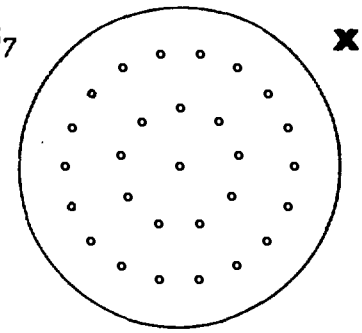

1.3447
1 9 18

29_1

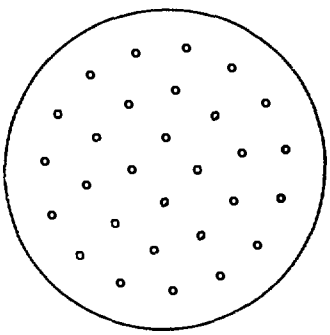

.3116
4 10 15

29_2

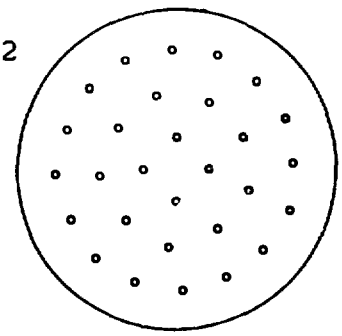

.3234
4 9 16

29_3

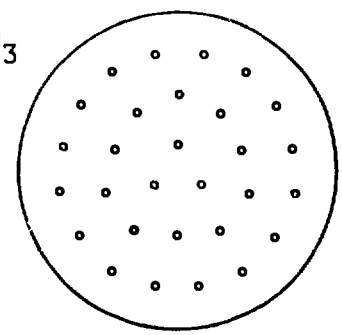

.3460
3 3 7 16

29_4

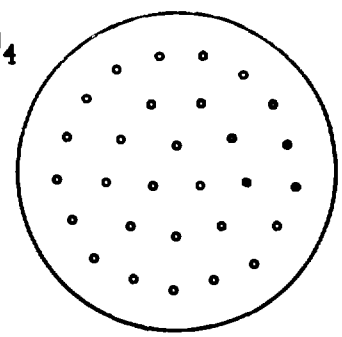

.4599
3 3 6 17

30_1

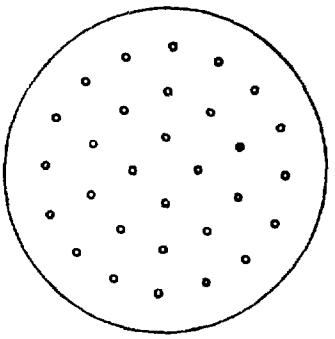

.2767

4 4 6 16

30_2

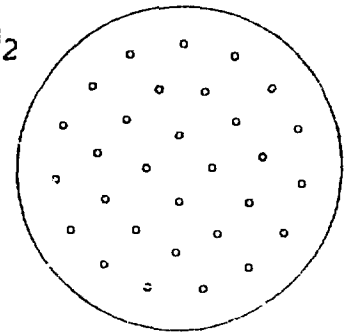

.3943

4 11 15

30_3

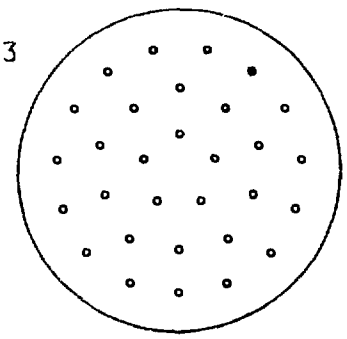

.4059

5 5 5 15

30_4

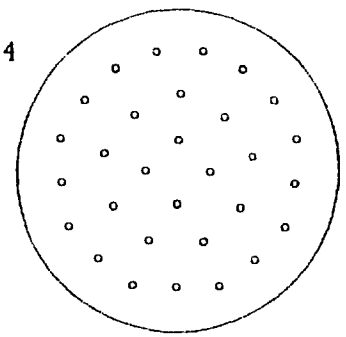

.4074

4 9 17

30_5

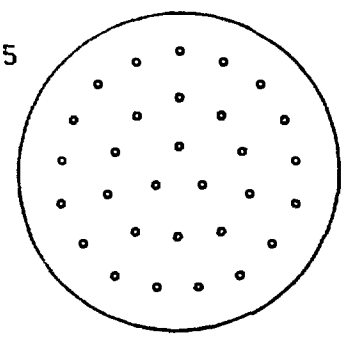

.4354

3 3 7 17

37_1

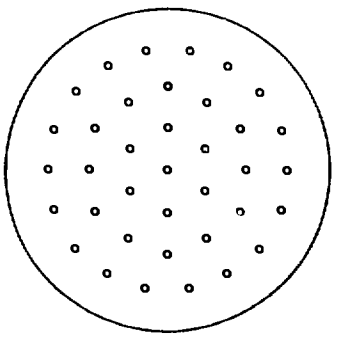

.2842

1 6 6 6 18

37_2

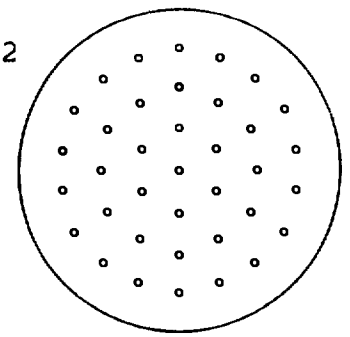

.2888

1 6 6 6 18

37_3

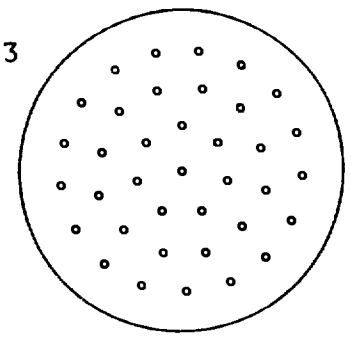

.3985

1 7 12 17

37_4

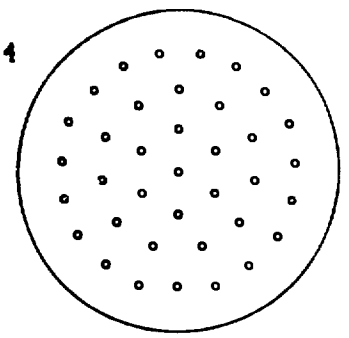

.4198

1 6 11 19

50_1

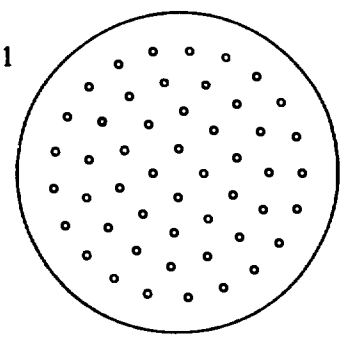

.4416

4 10 15 21

50_2

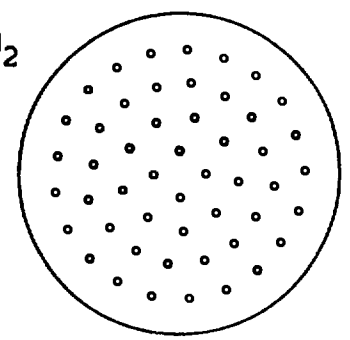

.4524

4 9 16 21

50_3

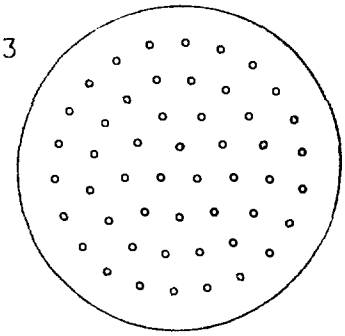

.4648

3 3 6 16 22

50_4

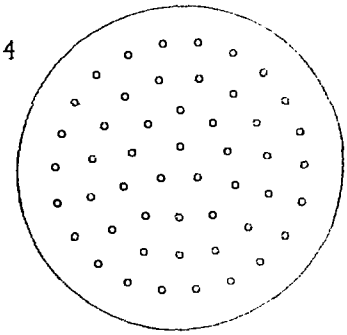

.4802

3 3 7 15 22

50_5

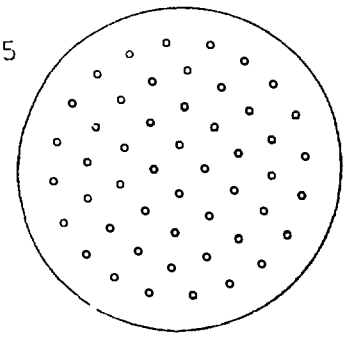

.4919

4 4 6 16 20

50_6

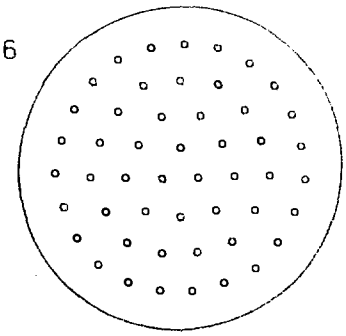

.5432

3 3 6 9 6 23

50_7

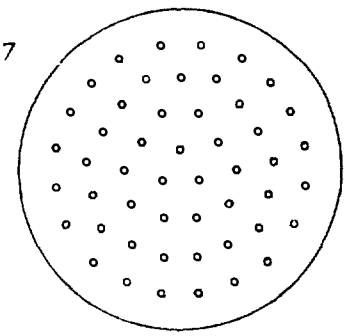

.6207

3 2 2 6 17 20

61_1

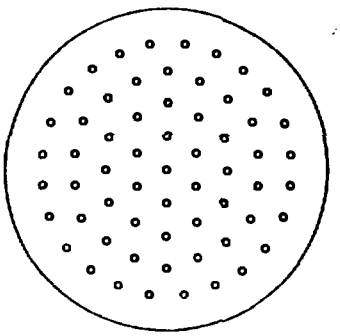

.3976

1 6 12 18 24

61_2

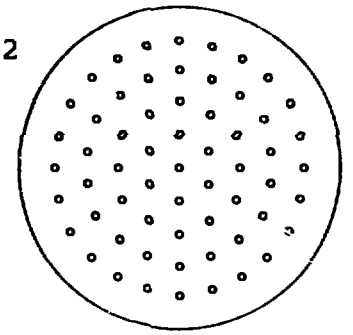

.4217

1 6 12 18 24

91_1

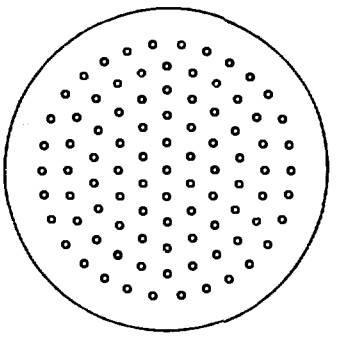

.5368

1 6 12 18 24 30

91_2

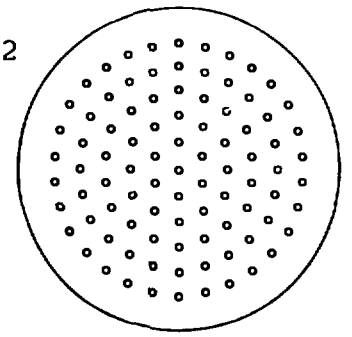

.5863

1 6 12 18 24 30

127_1

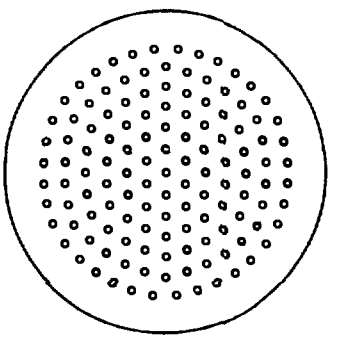

.7035

1 6 12 18 24 30 36

127_2

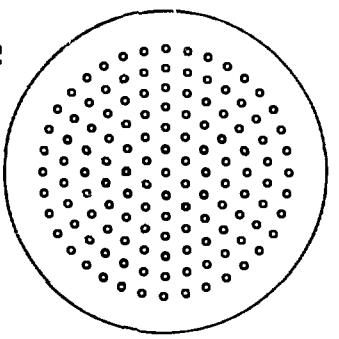

.7829

1 6 12 18 24 30 36

169_1

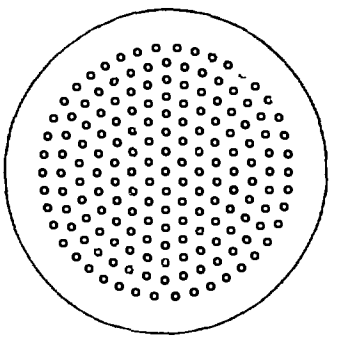

.8983

1 6 12 18 24 30 36 42

169_2

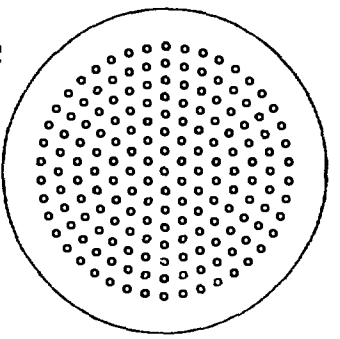

1.0117

1 6 12 18 24 30 36 42

217_1

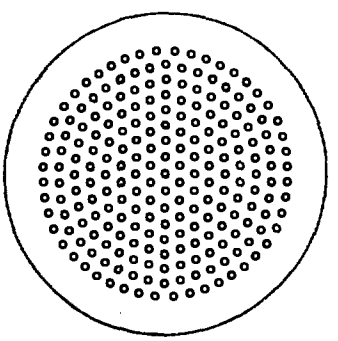

1.1221

1 6 12 18 24 30 36 42 48

217_2

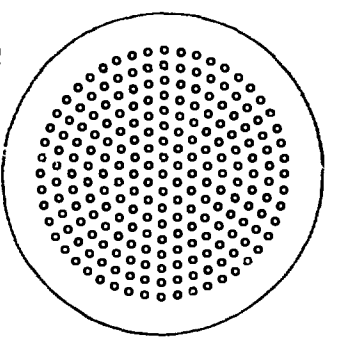

1.2725

1 6 12 18 24 30 36 42 48

REFERENCES

1. T. H. Havelock, "Stability of Motion of Rectilinear Vortices in Ring Formation," Phil. Mag. XI, 617-633 (1931).
2. G. B. Hess, "Angular Momentum of Superfluid Helium in a Rotating Cylinder," Phys. Rev. 161, 189-193 (1967).
3. D. Stauffer and A. L. Fetter, "Distribution of Vortices in Rotating Helium II," Phys. Rev. 168, 156-159 (1968).
4. L. M. Milne-Thomson, Theoretical Hydrodynamics (Macmillan, London, 1968), Chap. XIII, §13.50.
5. H. Lamb, Hydrodynamics (Dover, New York, 1945), §157.